

Accepted Manuscript

Three-armed rifts or masked radial pattern of eruptive fissures? The intriguing case of el hierro volcano (canary islands)

L. Becerril, I. Galindo, J. Martí, A. Gudmundsson

PII: S0040-1951(15)00080-3
DOI: doi: [10.1016/j.tecto.2015.02.006](https://doi.org/10.1016/j.tecto.2015.02.006)
Reference: TECTO 126541

To appear in: *Tectonophysics*

Received date: 22 September 2014
Revised date: 30 December 2014
Accepted date: 10 February 2015



Please cite this article as: Becerril, L., Galindo, I., Martí, J., Gudmundsson, A., Three-armed rifts or masked radial pattern of eruptive fissures? The intriguing case of el hierro volcano (canary islands), *Tectonophysics* (2015), doi: [10.1016/j.tecto.2015.02.006](https://doi.org/10.1016/j.tecto.2015.02.006)

This is a PDF file of an unedited manuscript that has been accepted for publication. As a service to our customers we are providing this early version of the manuscript. The manuscript will undergo copyediting, typesetting, and review of the resulting proof before it is published in its final form. Please note that during the production process errors may be discovered which could affect the content, and all legal disclaimers that apply to the journal pertain.

**THREE-ARMED RIFTS OR MASKED RADIAL PATTERN OF ERUPTIVE
FISSURES? THE INTRIGUING CASE OF EL HIERRO VOLCANO (CANARY
ISLANDS)**

L. Becerril^{1,2}, I. Galindo², J. Martí¹, A. Gudmundsson³

1) Institute of Earth Sciences Jaume Almera, ICTJA-CSIC, Group of Volcanology. SIMGEO (UB-CSIC) Lluís Solé i Sabarís s/n, 08028, Barcelona, Spain.

2) Spanish Geological Survey (IGME), Unit of Canary Islands, Alonso Alvarado, 43, 2ºA, Las Palmas, 35003, Spain.

3) Department of Earth Sciences, Royal Holloway University of London, Egham, TW20 0EX, UK.

Corresponding author: Laura Becerril (laurabcar@gmail.com)

HIGHLIGHTS

- The first comprehensive volcano-tectonic model of El Hierro
- New analysis of the structural elements: vents, eruptive fissures, dykes and faults
- Structural-element distribution suggests uniform stress field during construction
- Shallow NE, S, and W rifts indicate local stress fields conditioned by landslides

Abstract

Using new surface structural data as well as subsurface structural data obtained from seventeen water galleries, we provide a comprehensive model of the volcano-tectonic evolution of El Hierro (Canary Islands). We have identified, measured and analysed more than 1700 volcano-structural elements including vents, eruptive fissures, dykes and faults. The new data provide important information on the main structural patterns of the island and on its stress and strain fields, all of which are crucial for reliable hazard assessment. We conducted temporal and spatial analysis of the main structural elements, focusing on their relative age and association with the three main cycles in the construction of the island: the Tiñor Edifice, the El Golfo-Las Playas Edifice, and the Rift Volcanism. A radial strike distribution, which can be related to constructive episodes, is observed in the on-land structures. A similar strike distribution is seen in the submarine eruptive fissures, which are radial with respect to the centre of the island. However the volcano-structural elements identified onshore and reflecting the entire volcano-tectonic evolution of the island also show a predominant NE-SW strike, which coincides with the main regional trend of the Canary Archipelago as a whole. Two other dominant directions of structural elements, N-S and WNW-ESE, are evident from the establishment of the El Golfo-Las Playas edifice, during the second constructive cycle. We suggest that the radial-striking structures reflect comparatively uniform stress fields during the constructive episodes, mainly conditioned by the combination of overburden pressure, gravitational spreading, and magma-induced stresses in each of the volcanic edifices. By contrast, in the shallower parts of the edifice the NE-SW, N-S and WNW-ESE-striking structures reflect local stress fields related to the formation of mega-landslides and masking the general and regional radial patterns.

Keywords: Volcano-structure, El Hierro, Canary Islands, dyke, eruptive fissure, radial distribution

1. Introduction

Understanding structural controls of volcanic systems is of great importance in order to characterise their volcano-tectonic evolution and internal structure. Ideally, volcano-tectonic studies should include field studies that provide information on dykes, faults, joints, eruptive fissures and alignments (inferred lineament strike) of eruptive centres. Also needed are geophysical studies that provide knowledge about the deep structure of a volcano using various techniques such as gravimetry, seismic refraction or reflection, magnetotellury, and seismic tomography.

The reconstruction of the tectonic evolution of a volcanic system is commonly made more difficult by the critical evidence as to the relationship between volcanism and tectonic stress-fields often being obliterated or masked by the later volcanic and tectonic processes. This problem may be compensated for by geophysical imaging that may provide valuable information on the internal structure of the volcanic system, although the resolution of geophysical methods is not always sufficient to identify volcano-tectonic structures such as the deeper expressions of dykes or eruptive fissures (Fiske and Jackson, 1972; McGuire and Pullen, 1989; Gudmundsson, 1995; Acocella et al., 2006; Neri et al., 2011).

The most common volcano-tectonic studies are based on compilations of surface structural data which may, or may not, be compared with available geophysical data. In particular, the location and orientation of dyke swarms provide important information on the existing stress field at the time of their emplacement (Pollard et al., 1983; Gudmundsson, 1995; Marinoni and Gudmundsson, 2001). Systematic studies of dykes

have been carried out by several authors as one of the best methods for exploring the paleostress fields and their variations in space and time (Pollard et al., 1983; Gudmundsson, 2003). Furthermore, other structural elements in volcanoes, such as eruptive fissures, alignments of vents, faults, and other fractures, make it possible to deduce the main structural patterns of a volcanic area and indicate the past and recent paths of the magma in its ascent to the Earth's surface. The compilation and analysis of the information on all these elements is the first step for understanding the tectonic evolution of a volcanic area.

Linear volcanic alignments and associated dykes are commonly perpendicular to the least compressive stress (Anderson, 1936; Nakamura, 1977; Delaney et al., 1986). Feeder-dykes, in particular, underline the structural trends of past eruptions (Galindo and Gudmundsson, 2012). Faults, extension fractures, eruptive fissures and lineaments deduced through elongated cones and volcanic vents provide an opportunity to use them as a means to map stress fields in volcanic areas (Nakamura, 1977; McGuire and Pullen, 1989; Connor et al., 1992; Tibaldi, 1995; Marinoni and Gudmundsson, 2000). The orientation of these volcano-structures serves as an indicator for the average direction of tectonic stresses in the upper crust at the time they formed.

Several volcano-structural studies have been carried out during the last decades in the Canary Islands, in a general way (Feraud et al., 1985; Stillman, 1987; Carracedo, 1994), and on some of the islands in particular: Fuerteventura (Ancochea et al., 1996; Ahijado et al., 2001); Lanzarote (Marinoni and Pasquarè, 1994); Gran Canaria (Schmincke, 1967; Hernán and Vélez, 1980; Schirnack et al., 1999); Tenerife (Carracedo, 1996; Martí et al., 1996; Marinoni and Gudmundsson, 2000; Galindo, 2005; Galindo et al., 2005; Geyer and Martí, 2010; Galindo and Gudmundsson, 2012); La Gomera (Hernán et al., 2000; Ancochea et al., 2003, 2008); La Palma (De la Nuez,

1984; Fernández et al., 2002). These studies have mainly focused on the analysis of dyke swarms and rarely on eruptive fissures and faults.

In El Hierro the first studies were mainly concerned with depicting of general tectonic elements and fractures on the island (Hausen, 1964; Coello, 1971). In 1977, Pellicer developed the first schematic volcano-structural map, including eruptive vents and lineaments. This was further refined and added to by Navarro and Soler (1995) who analysed the island's main volcano-structural elements, paying special attention to the distribution of dykes, particularly inside water galleries. Day et al. (1997) focused on the main fault system of the island, which was also mapped as regards the general outline by IGME, 2010a. Other works have been mainly focused on the exploring the geologic and tectonic evolution of the island (Carracedo, 1996; Carracedo et al., 2001; IGME, 2010a-d). Münn et al. (2006) used scaled analogue experiments to reproduce the geometry of rift zones and the unstable flanks observed on El Hierro and to associate them with gravitational volcano spreading. Also, Manconi et al. (2009) suggested that the stress perturbation caused by the formation of the largest and most recent of these flank collapses—the El Golfo landslide—likely influenced the magma plumbing system of the island, leading to the eruption of a higher proportion of denser and less evolved magmas.

With the aim of obtaining a comprehensive picture of the tectonic evolution of the island, and to understand the role of rift zones and large landslides in its evolution, we have carried out a detailed volcano-tectonic study of El Hierro. El Hierro hosts very accessible outcrops that have been revealed by the erosion of the island's oldest ravines and gravitational landslides, which enable the subaerial parts of the island to be studied in great detail. Moreover, as in other Canary Islands, a large number of subhorizontal water tunnels have been dug on El Hierro, which offers the opportunity to study the

internal structure of the volcanic edifice. To conduct the corresponding spatial and temporal analysis of the main volcano-structural elements, including subaerial and submarine vents and eruptive fissures and dykes, we analysed separately the three main cycles in the construction of the island. These three cycles are represented by the: (1) the Tiñor Edifice, (2) the El Golfo-Las Playas Edifice, and (3) the Rift Volcanism (Guillou et al., 1996; IGME, 2010a-d). Faults are described and analysed separately. Part of this study has already been used in a volcanic susceptibility analysis of the island (Becerril et al., 2013a). In this paper, we concentrate on the information that the analysed structural elements provide as to the local and regional stress fields and their cause/effect relationships with the rift zones and large landslides.

2. Geological and Tectonic Setting, and structural elements of El Hierro

The Canary archipelago (Spain) is located 100 km off the Northwest African coast, which extends for roughly 500 km in a chain that has developed on the passive margin of the African Plate in the eastern central Atlantic Ocean (Inset A in Figure 1). This archipelago is the result of a long volcanic and tectonic activity that started at around 60 Ma ago (Robertson and Stillman, 1979; Le Bas et al., 1986; Marinoni and Pasquarè, 1994; Marinoni and Gudmundsson, 2000).

Few tecto-volcanic structures have been recognised and described in the Canarian archipelago from seismic exploration and marine geophysical studies (Figure 1, inset B). These have revealed different crustal structures on the lithosphere of the Canary Islands (Bosshard and McFarlane, 1970; Mezcua et al., 1992; Banda et al., 1981; Carbó et al., 2003).

Main fractures in the islands and ocean floor may be classified in two types or families (Hérendez-Pacheco and Ibarrola, 1973): Atlantic “oceanic” (N160–N180°E,

N120–N135°E) and African “continental” (strikes: N20°E, N45°E, N75°E), depending on their relation with the opening of the Atlantic or the tectonics of the Atlas range in the African continent, respectively (Fuster, 1975; Anguita and Hernan, 1975, 2000; Emery and Uchupi, 1984; Dañobeitia, 1988; Geyer and Martí, 2010). In this sense, the eastern islands form a very conspicuous NE-SW structure, the so-called East Canary Ridge, whereas the western islands structures show a general N-S trend.

El Hierro, the south-western most and youngest of the Canary Islands with an oldest subaerial rocks of only 1.12 Ma (Guillou et al., 1996), represents the emergent part of a volcanic edifice which rises 5500 m from the sea bottom. Its subaerial part emerges 1501 m a.s.l. and it has a surface area of about 269 km² (Figure 1). Its morphology has been moulded by three amphitheatres (El Golfo, Las Playas and El Julan) that correspond to the headwall scarps of giant landslides (Masson, 1996; Urgeles et al., 1996, 1997; Carracedo et al., 1999, 2001; Masson et al., 2002; Longpré et al., 2011).

Three main constructive cycles are known as (1) the Tiñor Edifice (1.12–0.88 Ma), (2) the El Golfo-Las Playas Edifice (545–176 ka), and (3) the Rift Volcanism (158 ka–Present) (Guillou et al., 1996; Carracedo et al., 2001; IGME, 2010a-d). These cycles have been the main contributors to the growth of the island, and have been separated by periods of quiescence, erosion and sector collapse. The Tiñor Edifice mainly crops out in the incised valleys and cliffs of the NE-part of the island (Figure 1). El Golfo-Las Playas Edifice was constructed as an attachment to the western flank of the remnants of the previous edifice. The rocks generated by this cycle can be examined on the landslide escarpments of Las Playas and El Golfo, and also on the west and southeast cliffs of the island (Figure 1). The last growing stage of El Hierro has been characterised by a structural configuration controlled by an apparently three-armed rift zone system (since

158 ka) (Guillou et al., 1996; Carracedo et al., 2001). This last cycle is distinguished by relative compositionally homogeneous volcanic products, mainly forming scoria cones and mafic lava flows emitted from eruptive fissures along the island's three rifts (Figure 1).

At least six giant landslides have occurred during the construction of the subaerial part of El Hierro. The most recent ones are Las Playas I and II (~ 545-176 ka and 176-145 ka, respectively), El Julan (> 158 ka), and El Golfo (~ 87-39 ka) (Masson, 1996; Gee et al., 2001b; Masson et al., 2002; Longprè et al., 2011). Another landslide also affecting the Tiñor Edifice has been proposed at around 0.8 to 0.5 Ma (Carracedo et al., 2001; IGME, 2010 a, c). The oldest landslide has been proposed for the first stages of the subaerial construction of the island, probably between 1.12 and 1.04 Ma, affecting the northern side of the Tiñor Edifice (IGME, 2010 a, c). The superposition of constructive and destructive episodes has led to a complex internal structure in El Hierro, which can be identified in part along the direct exposures created by erosion and/or landsliding and in the water tunnels. The uppermost part of the feeding system forms a sheet intrusion complex in which inclined sheets (mostly dipping 80-90°) developed preferentially following NE, W and S trends parallel to the rift systems (Carracedo et al., 2001).

Volcanic vents and eruptive fissures are the most recognisable elements on the island and can be also identified in the surrounding submarine areas. In fact, El Hierro is the island with the highest number of monogenetic volcanoes per km² of the Canary Islands (more than 220 cones corresponding to the Rift Volcanism). Subaerial vents are distributed mainly along the rifts, and only a few of them are located inside the landslide valleys. Submarine eruptive vents are common around the island, except

within the submarine landslide valleys, where only a few emission centres have been inferred.

Eruptive fissures defined by the alignments of volcanic vents are mainly observed in the rift zones; most have the same trend as their associated rift (Figure 2b). By contrast, the submarine fissures display a radial distribution with respect to the centre of the island (Figure 2a) (Becerril et al., 2013a). Most of the onshore fissures are related to the last cycle of activity of El Hierro (the past 158 ka) and are often partially buried by lava flows, thus representing portions of originally more extended lineaments.

Faults are mainly recognisable on the island's NE rift, where a graben system has been identified (IGME, 2010a). These faults are well exposed with steeply dipping planes striking NE-SW (Day et al., 1997). In the southern and western rifts a few outcropping faults show N-S and E-W strikes, respectively. There are also normal faults running parallel to the scarp of El Golfo, some of which are gaping, that is, open fractures. These latter, however, are not related to regional tectonics but rather associated with the more local sector collapses.

3. Methodology

Extensive field work and geological revision of the interior of seventeen water galleries (sub-horizontal water tunnels) were conducted in order to identify and measure the main volcano-structural elements, such as vents, eruptive fissures, dykes and faults. Structural mapping was performed with the software ArcGIS 9.2 by ESRI© at a scale of 1:25000 using ortophotographs (1:5000) and high-resolution coloured aerial photographs (1:18000) from GRAFCAN (www.grafcan.com). The digital geological map from the Spanish Geological Survey (IGME, 2010a-d) (1:25000) (<http://cuarzo.igme.es/sigeco/>), the LIDAR Digital Elevation Model (1:5000) from the

National Geographic Institute (IGN) (<http://centrodedescargas.cnig.es/CentroDescargas/index.jsp>), bathymetrical data from the Spanish Institute of Oceanography (IEO) (<http://www.ideo-elhierro.ieo.es>) and Somoza et al. (2012) were also used, in these last cases to infer submarine vents and eruptive fissures. A spatial database was built to host the volcano-structural data derived from the fieldwork and the geological analysis (Becerril et al., 2009; Bartolini et al., under review). All the studied structural elements were georeferenced in UTM 28 N-WGS84.

Subaerial vents were mapped in the following way (cf. Becerril et al., 2013a): (1) as individual points placed at the centre of craters of isolated cinder cones, (2) as craters of coalescent cinder cones, (3) as craters without an associated cinder cone and also (4) as vents that belong to hornitos and spatter ramparts. Regarding submarine eruptive vents, only those that are morphologically recognisable as volcanic cinder cones were considered, and were mapped as individual points corresponding to their summits.

Eruptive fissures were identified through the alignment of two or more vents that forming part of coalescent craters-cones or, alternatively, one vent defining an elliptical crater. The latter were defined when the cinder cone rims were completed and constructed in slopes less than 4° to avoid slope effects (Tibaldi, 1995). In those cases where cinder cone rims were incomplete, we constructed the best-fit ellipses and calculated the axial ratios for each vent (Paulsen and Wilson, 2010). Each eruptive fissure was reported as a lineament linking the volcanic vents opened during the same eruption. Eruptive fissures length, strike and associated number of vents were compiled in the database.

In the case of dykes, strike, dip and thickness were measured, as well as the intrusive relationships with the host-rocks (chilled margins, its thickness) and petrological aspects (composition, texture). Geochemical analysis were performed and projected on a TAS diagram (see details in the Electronic Supplementary Material). Strike values were corrected taking into account the magnetic declination at the time of measurement ($\sim 7^\circ$), (International Geomagnetic Reference Field (IGRF) <http://wdc.kugi.kyoto-u.ac.jp/igrf/>). Data on strikes and dips are given to an accuracy of about 5° . The thickness accuracy is about one order of magnitude smaller than the measured value, that is, about 10%. Apparent dyke thicknesses data in the water galleries were corrected bearing in mind the water gallery azimuth. Gallery lines rather than the dyke direction (due to their small scale) are depicted on the maps. Dykes were first analysed according to their relation to each of the volcanic cycles identified in the evolution of the island, and second according to their location. Eruptive fissures were included in the dyke analyses since the fissures are considered the surface expression of feeder-dykes.

Preliminary ortophoto interpretation was carried out in order to check previously mapped faults (Coello, 1971; Pellicer, 1977; Navarro and Soler, 1995; Day et al., 1997; Carracedo et al, 2001; IGME, 2010a-d) and to identify new ones. Populations of fault-slip data were collected in the field at different sites to reconstruct the paleostress field. Strike, dip and pitch of slickensides were measured. Where breccia and fault polish were visible, measurements and description of them were also made and recorded. Some faults crop out in inaccessible cliffs, in which case the fault strike was measured from the map and the fault dip considered subvertical. Kinematic study of faults was performed using FaultKin5 free software (Allmendinger et al, 2012). The structural analysis of faults was conducted separately from that of dykes and eruptive fissures.

Stereograms of eruptive fissures, dykes and faults were performed for each area. Rose and contour diagrams were derived using the software Stereonet 8 (Allmendinger et al, 2012). Histograms of strikes, dips and thicknesses were processed for analysis of the data with Microsoft Excel 2010 (Microsoft).

4. Description of the El Hierro volcano-structural elements

In order to have an overview and to comprehend the patterns and characteristics of the structural elements of El Hierro, in this section we describe each volcano-structural element separately before making the structural analysis, except for faults whose description and analysis are presented together in section 6.

4.1 Vents and Volcanic Fissures (Onshore and Offshore)

More than 900 vents were mapped, of which 67% are onshore vents and the remainder 33% offshore vents (Figure 2a, Table 1). Onshore vents are more abundant in the central parts of rift zones, mainly forming part of the Rift Volcanism edifice (94% of vents). NE, S and W rifts have similar percentages of vents (Table 1). Other than within the submarine parts of the landslide valleys, where only a few centres have been identified, submarine vents are common around the island (Figure 2a). Offshore vents could not be attributed to any particular stage of construction of the island due to the lack of geochronological and stratigraphic information, except those of the 2011 eruption. 60% and 67% of vents onshore and offshore respectively were used to delineate volcanic fissures.

Onshore Volcanic fissures are basically recognisable along the rift zones (Figure 2b). A total of 126 eruptive fissures were identified on the island: six on the Tiñor

Edifice and the rest on the Rift Volcanism (Table 2). Of these, 56 are located on the NE rift, 34 on the S rift, 31 on the W rift, as well as five inside the El Golfo embayment. The majority of volcanic fissures (79%) were defined by two or three vents, but eruptive fissures with 4 to 33 vents were also delineated. The longest onshore eruptive fissure was measured at 2825 m on the NE rift of the Tiñor Edifice, while the shortest (~ 40 m) is located on the S rift belonging to the Rift Volcanism (Table 2). Those identified in the submarine areas reach lengths in excess of 4600 m length, while the minimum measured length is less than 100 m (Table 2). These eruptive fissures display a radial distribution with respect to the centre of the island (Becerril et al., 2013a). As for the vents, offshore eruptive fissures could not be attributed to any particular constructional episode due to the lack of specific information. Nevertheless, we grouped them according to their location being a total of 71 eruptive fissures: 37% on the NE rift, 41% on the S rift and 22% on the W rift (Table 2).

4.2 Dykes

A total of 587 dykes were studied in detail, 251 at the surface and 336 in the water galleries or tunnels (Figure 3a). Simple, multiple and composite dykes were observed (Figure 3b, c, d). The percentage of multiple and composite versus simple dykes is very low (less than 5%), implying that some 95% of the dykes are formed in single injections. Ten feeder dykes were identified; five of them were previously described by Becerril et al. (2013b) as feeders connected to their eruptive fissures (Figure 3e). Most dykes are massive in morphology (Figure 3f), and display columnar joints perpendicular to their cooling margins (Figure 3g). The general attitude (strike and dip) of individual dykes is usually constant at the outcrop scale, but local changes in strike, dip or both were sometimes observed (Figure 3). These changes in attitude can

occur at the boundary between two layers of different mechanical properties, such as between stiff (high Young's modulus) lava flows and less stiff or more compliant materials such as pyroclastic or sedimentary layers. Local rotation of the principal stresses can also occur within a single layer; for example, when moving from a massive and stiff central part of an aa lava flow to its compliant top and bottom scoria parts. Such a rotation largely explains the commonly observed en-echelon or segmented patterns in dykes and volcanic fissures (Figure 3h, k). Sometimes dykes split into two branches with different strikes (Figure 3i). Dykes generally tend to be parallel to each other (Figure 3j). Cross-cutting relationships between dykes can be occasionally observed, but the statistical data is insufficient to infer relative ages between different dyke populations (Figure 3l). Dykes thickness ranges from 0.1 m up to 12.5 m. We identified different dyke compositions. Most of the dykes have phenocrysts, mostly plagioclase-rich, olivine-rich, pyroxene-rich or ankaramitic. Previous geochemical analyses (Pellicer, 1977, 1979; IGME, 2010a-d) and the new ones show that dyke compositions are mainly tephri-basanites (42%), basalts (21%), and trachy-basalts (17%). Other basic compositions are represented by foidites (8%) and picrobasalts (4%). Few dykes show more evolved composition: trachyandesite (4%) and trachyte (4%) (Figure 1 in supplementary material).

5. Temporal and spatial analysis of dykes and eruptive fissures

To improve our knowledge of the island's volcano-tectonic evolution, we analysed the distribution of dykes and onshore and offshore eruptive fissures in relation to the different growth stages or edifices identified by previous studies (Guillou et al., 1996; Carracedo et al., 2001; IGME, 2010a-d). We analysed the relative stratigraphy of the island and grouped each different unit according to the edifices proposed by IGME

(2010a-d), and considered the different groups of dykes and eruptive fissures in terms of their stratigraphic level of emplacement. This gave us, in addition to the spatial distribution of the structural elements, a first order approach on their relative ages. This worked well for structures cropping out onshore both at surface and in the water galleries. However, the relative age estimates for the offshore structural elements (only eruptive fissures) was not possible due the lack of stratigraphic information. Dyke swarms are the most representative feature associated with Tiñor and El Golfo-Las Playas edifices. By contrast, few dykes were identified belonging to the Rift Volcanism, being eruptive fissures the most characteristic elements for the structural evolution study of this last constructive period. For the offshore area surrounding El Hierro, only eruptive fissures were analysed.

5.1 The Tiñor Edifice

A total of 183 dykes and 6 eruptive fissures were identified as belonging to edifice's constructive episode, which represent 31% and ~5% respectively, of the total of these types of structural elements identified in this study (Figure 4; Tables 2, 3). Concerning strike, dykes present two prevailing families: N40°-N60° and N170°-N180° (Figure 4a; Figure 7a, b; Table 3). At the head of the ravines (i.e. the highest emerged parts of the Tiñor edifice), the strike family N40-N60° predominates over the rest of directions. Despite the prevalence of these two orientations, dykes at the basal part of the edifice are radially distributed (Figure 4a). Eruptive fissures have a mean strike of N47° with just an E-W trend that is typical of the west rift (Figure 4b; Figure 7c; Table 2).

Most dykes are subvertical, with an average dip of 83° (Figure 4c, Table 3). The strike-dip angle relation (Figure 4e) shows that subvertical dykes dip in almost all

possible directions. Dykes thicknesses are between 0.5 m and 6.85 m, with a mean thickness of 1.45 m and mode (most common) thickness of 0.5-1 m (Figure 4d, Table 3). Figure 4f compares strike and thickness data, showing that the greatest thicknesses occur along the dominant strike directions N50° and N180°. The relation between dip and thickness (Figure 4g) shows that dykes dipping 80-90°, that is, subvertical dykes are the thickest.

Eruptive fissures length varies from 338 m to 2825 m, with the commonest lengths being between 500 and 1500 m (Figure 4h, Table 3).

5.2 El Golfo-Las Playas Edifice

A total of 328 of the studied dykes (56% of total) dissect the deposits of El Golfo-Las Playas Edifice. Strike values define two main swarms, N60°-N80° and N110°-N140°, showing much fewer dykes with the less representative directions of N10°-N60° or N150°-N180° (Figure 5a; Figure 7a,b; Table 3). Dips range from 60° to 90°, with most dykes being close to vertical, (Figure 5b, Table 3). Most dykes are less than 1 m thick, but the range is from a few cm to 12.5 m, with an average value of 1.6 m (Figure 5c, Table 3). The thickest dykes are close to vertical (Figure 5d). The relationship between strike and thickness reveals a large degree of dispersion. Nevertheless, it is clear that the thickest dykes are parallel to the main swarms (Figure 5f). No eruptive fissures were recognised as belonging to this edifice.

5.3 Rift Volcanism

76 dykes, representing 13% of the total number of dykes studied, belong to this edifice, while it contains 95% of the eruptive fissures (121 fissures) (Figure 6; Figure 7; Table 2, 3). The strikes of dykes and eruptive fissures agree with the trend of each rift.

The majority of dykes follow three main strike directions, namely N40°-N50°, N100°-N130° and N160°-N180°, whereas those of the eruptive fissures are N52°, N89° and N145°. These strike directions of dykes and fissures coincide roughly with the trends of the northeast, west and south rifts (Becerril et al., 2013a) (Figure 6a, b; Figure 7a, b).

Most dykes are subvertical, with a dip average value of 83° (Figure 6c). 77% of the dykes have thickness between 0.5 m and 1.5 m, the mean being 1.3 m (Figure 6d, Table 3). Moreover, the relationship between strike and dip shows that vertical dykes follow all the three main strikes (Figure 6e). The thickest dykes are primarily related to west and south rift directions, but thinner dykes, less than 1.5 m thick, occur in all the three rifts (Figure 6f). Figure 6g shows that the thicker dykes are generally steeply dipping, that is, close to vertical.

Figure 6h shows eruptive fissures length onshore that range from 38 m to 1557 m, the most common (mode) length roughly between 200 and 800 m (Table 2).

5.4. Offshore structures

The analysed offshore structures correspond to apparent eruptive fissures for which relative stratigraphy and age is not known. We can only provide a relative age for the eruptive fissures observed in the landslides valleys, that is, they are younger than the landslides. A sector-by-sector analysis of offshore fissures indicates three main strike directions when they are averaged together in each sector, namely N061° in the northeastern sector, N161° in the southern sector, and N30° to N126° (Figure 7c) in the western sector. These directions coincide with the onshore rift trends. However, when taken together, the offshore eruptive fissures define a radial pattern from the emerged part of the island (Figure 2b). Focusing the attention on the distribution of eruptive fissures on the offshore continuation of the western rift zone, their arrangement spreads

partially radially from N70° to N140°. This spread in strike is also observed, although less clear, in the eruptive fissures located upwards and around Las Playas valley, that strike from N45° to N150°. This wider distribution is less apparent in those areas affected by landslides (Figure 2b), but inside el Julan, one of the oldest landslides, they show a clear radial distribution.

6. Faults

32 faults were identified and mapped on the island; most of which are exposed but few covered by soil, vegetation and lava flows. All the faults have a clear normal component and dipping fault planes. Measured fault lengths range from about one hundred meters to several kilometres, but the estimated length depends partly on how well exposed the faults are. They outcrop mainly along the Tiñor Edifice and only a few faults dissect the youngest edifice, i.e., the Rift Volcanism (Figure 8).

In the NE rift, faults display a graben system, nearly 6 km long and 1.5 km wide (Figure 8). Towards the south, there are indications of buried normal faults (dissecting the Las Playas scarp) which are also associated with the graben, in which case graben may be as long as 10 km. Some parts of these faults are covered by younger lava flows. The graben is bounded by two major normal faults striking ENE-WSW. The largest one is the northwestern fault which reaches a strike dimension of 5.8 km (Figure 8). The southeastern boundary fault has a discontinuous exposure and represents the antithetic fault to the northwestern boundary fault. Inside the graben, up to three smaller antithetic faults were recognised through photo-interpretation since they do not have clear morphological expressions in the field (Figure 8). The northwestern boundary fault dips an average of 65° to SE and the height of its escarpments, and thus the minimum throw,

is about 30 m. These faults were previously studied and referred to as the “San Andrés fault system” by Day et al. (1997), Carracedo et al. (2001) and IGME (2010a)..

Other faults were identified on the Las Playas escarpment and also in the southernmost part of the island. They are normal faults and display N-S and NNW-SSE strikes. At the western rift, few normal faults were located in the southwest area, striking E-W (Figure 8). These are represented by morphological escarpments partly buried by recent lavas. On the El Golfo scarp edge seven normal faults were identified (Figure 8). They are parallel with the scarp and dip towards the embayment. The estimated vertical displacement or throw is about 10 meters.

Figure 8 corresponds to a rose diagram of the El Hierro faults. Two principal fault families striking NE-SW and WNW-ESE appear on the island, the former being the most prominent. Faults associated with the graben system, in the northeast part of the island, show in the rose diagram a clear NE-SW direction (Figure 8, Table 4). Towards the northeast, the main fault of the graben shows a slightly change in strike, that is, to E-W direction and affecting Mt. Los Picos (Figure 8, Table 4). This change in strike is reflected in the following: in an outcrop found in the old road of Tiñor (Station 0 in Figure 8, Table 4), the fault attitude is $040^{\circ}/65^{\circ}\text{SE}$. But towards the northeast (Station a in Figure 8, Table 4) the attitude changes first to $067^{\circ}/65^{\circ}\text{SE}$ while in Mt. Los Picos (Station b and c in Figure 8, Table 4) and then to the fault changes its attitude to $090^{\circ}/72^{\circ}\text{SE}$. Along the exposed plane of the graben main fault slickensides are observed. At stations 0, a and b (Figure 8) we measured slickensides showing plunge at 65° towards 135° , 62° towards 130° and 60° towards 139° , respectively.

7. Discussion

In ocean volcanic islands, the presence of rifts zones and large sector collapses is common and several theories/models have been proposed to explain the organisation of the main volcanic intrusions along rifts and their relation to sector collapses. Existing models are based on: (1) topographic and gravity-control (Fiske and Jackson, 1972); (2) intense intrusive activity or magma-induced upwelling along volcanic rifts that can trigger sector collapse (Dieterich, 1988; Carracedo, 1994); (3) structural changes induced by dyke intrusions (Walker, 1992); (4) gravitational spreading controlled by the volcano load, growth rate and the presence of one or more detachment planes that facilitate lateral sliding (Borgia et al., 2000 and references therein; Walter et al., 2006; Delcamp et al., 2011); (5) regional stress/strain fields and pre-existing oceanic structures (Geyer and Martí, 2010); and (6) landslides that trigger the reorganization of rifts and lead to their formation opposite the collapse embayment (Tibaldi, 1996, 2001; Acocella and Tibaldi, 2005; Walter et al., 2005). With all these models it is as yet unclear whether it is the intense intrusive activity or the sector collapses that actually control the structural evolution and geometry of oceanic rift zones (Delcamp et al., 2012 and references therein).

Two main hypotheses have been proposed to explain the apparent three-armed rift zones of El Hierro. The first explains that rifts development as a result of local stresses generated by the up-pushing action of updoming magma (Carracedo et al., 1996). The second suggests that gravitational spreading controls rift zones and flank instability (Münn et al., 2006). Furthermore, a third theory applicable to El Hierro proposes that the evolution and origin of the Canary Islands have been strongly controlled by regional tectonic structures (Geyer and Martí, 2010).

Different directions of intrusive sheeting and fracturing have been reported for the main structural elements on El Hierro island, mainly in the NE, S and W (Pellicer,

1977; Fuster, 1993; Carracedo et al., 2001; Münn et al., 2006; IGME, 2010a-d) and shown to strike roughly parallel with the rift zone within which they are located. On this view, the island has been referred to as a classic example of a three-armed rift system with three ridges arranging $\sim 120^\circ$ (Fuster et al., 1993; Carracedo, 1996; Carracedo et al., 1998, 2001). Submarine studies, however, have provided information about the offshore continuation of volcanic rift zones on El Hierro, where the distal south rift of the island has been interpreted as an old edifice, and not as a part of the southern propagating rift zone (Gee et al., 2001a; Schmincke and Graf, 2000; van den Bogaard., 2013), whereas NE and W submarine rifts are interpreted as seaward bifurcations of the onshore rift zones (Gee et al., 2001a).

Onshore volcanic fissures are basically recognisable in the rift zones, having an apparent general trend similar to that of the rift within which they are located (Becerril et al., 2013a). The present paper, however, shows that the structural elements on the entire volcanic edifice (subaerial and submarine) display a clear radial distribution with respect to the centre of the island (Figure 2b). The occurrence of landslides has modified the original distribution giving the appearance of a three-armed rift zone structure.

A radial pattern does not support the idea proposed by Gee et al. (2001b) who suggested for the offshore western and northeastern flanks seaward bifurcations or a broad zone of rifting continuous to the onshore rift zones. Therefore, the classic idea of a three-armed rift system with three ridges at 120° (Fuster et al., 1993; Carracedo, 1996; Guillou et al., 1996; Carracedo et al., 2001) generally does not fit well with this wider radial distribution.

Radial patterns of dykes and eruptive fissures in large volcanoes are assumed to reflect a stress field developed by an axially symmetric intrusion or magma chamber

and the effect of volcanic loading (Ode', 1957; Pollard, 1987; Fernández et al., 2002; Gudmundsson, 2006). However, in the presence of a tectonic stress field, the dyke pattern may deviate significantly from the radial geometry (Ode', 1957; Muller and Pollard, 1977; Nakamura, 1977), and particularly so when the host rock is heterogeneous and anisotropic (Gudmundsson, 2006). Radial patterns are also observed in developed volcanic edifices where lateral collapses have occurred, but normally where the injections are far enough from the unstable sectors (Walter, 2003). The observed radial distribution of the offshore fissures on El Hierro could be explained by the comparatively small influence that the landslides exerted on further intrusions, since radial offshore fissures are far enough from the unstable sectors. Moreover, the radial patterns of onshore fissures and dykes seem to support the existence of fairly uniform stress fields during the construction of the island's three edifices, being occasionally disturbed by the development of lateral collapses, rather than a persistent three-armed rift configuration, as proposed by previous studies (Carracedo 1994, 1996; Carracedo et al., 2001; Gee et al., 2001a). This suggests that the present rift system developed superficially as a consequence of the partial destruction of the edifice, and during the later stages in the construction of the island. Thus, these NE, W and S rift trends are probably resulting of local stress changes caused by the formation of the large landslides on the island.

The lateral migration of magma along the crustal/mantle boundary beneath the W rift, which occurred during the unrest episode preceding the 2011-2012 El Hierro eruption, also supports the shallow nature of these rift structures (Martí et al., 2013), which would only affect the uppermost part of the volcanic edifice, similarly to Kilauea Volcano in Hawaii (Ryan, 1988). However, in the case of El Hierro Volcano, the

confirmation of this assumption would require new geophysical studies such as tomography methodologies.

Following the eruption, seismic swarms indicating magma movement tended to migrate in different directions (to the west and northeast), crossing below the W and NW rift zones without leading to an eruption, thereby suggesting that the rift zones do not offer so much deep paths for magma to reach the surface.

Similar structural patterns showing a radial distribution of dyke swarms in subaerial volcanic edifices have been recognised in other oceanic islands and even in some of those from the Canary archipelago (De la Nuez, 1984; Chadwick and Howard, 1991; Ancochea et al., 1994, 2003, 2008; Fernández et al., 2002). Fernandina and Isabela (Galapagos), for example, show radial eruptive fissures that appear to result mainly from the interaction between local magmatic and gravitational stresses, modified to a minor extent by regional stresses (Chadwick and Howard, 1991).

Dykes following radial patterns have been described in La Palma, (De la Nuez, 1984; Ancochea et al., 1994, Fernández et al., 2002) and La Gomera (Ancochea et al., 2003, 2008 and references therein). The radial dyke swarm from La Palma is modified by a dominant northern trend (Staudigel et al., 1986), thereby reflecting the influence of a regional stress field affecting the lithosphere of the Canary Archipelago. Fuerteventura has subaerial edifices (aligned following regional trends) exhibiting radial dyke swarms (Ancochea et al., 1996).

In addition to the general radial distribution mentioned before, our data analysis also reveals a predominant NE-SW direction over time and space. Other dominant direction, N-S, is evident subsequent to the establishment of the El Golfo-Las Playas edifice. These directions that coincide with the rift trends, could be related to deep crustal structures that may be controlled principally by regional tectonic faulting

recognisable at the basement of the archipelago, which is also present on most of the other Canary Islands, as has been suggested by Geyer and Martí (2010 and references therein) (Figure 1, inset B). However, we cannot exclude the possibility of the NE structural direction being related to the generation of a lateral west collapse of the Tiñor Edifice, about 0.88 Ma ago (Carracedo et al., 2001; IGME, 2010a). As well, this could be the consequence of the already developed fault system with a NE-SW strike, corresponding to the onshore part of a large slump also observed offshore (Gee et al., 2001a), which could have conditioned the orientation and size of the last Tiñor Edifice eruptions. These structures may be related to the gravitational spreading of the first edifice that conditioned the formation of parallel faults on both sides of it, similar to those structures observed in analogue experiments on Hawaii and La Reunion by Walter et al. (2006).

In comparison with other Canary Islands such as Lanzarote or Tenerife (Marinoni and Pasquarè, 1994; Galindo et al., 2005), surface faults are less abundant on El Hierro, possibly because they are buried by recent deposits. The graben system studied on the NE of the volcanic edifice has been interpreted as an aborted inactive giant flank collapse (Day et al., 1997). This graben system has numerous faults parallel to the main one, which confirms the extensional nature of the graben. Although there is no evidence of interaction between faults and dykes in this graben, the presence of the biggest cinder cones around and along the graben (e.g. Ventejis, Los Picos), seems to indicate that the bounding faults favoured magma ascent and occurrence of larger eruptions. From other volcanic areas, it is known that dyke commonly use faults, both normal and strike slip faults, as part of their paths (Falsaperla et al., 2010; Neri et al., 2011; Cappello et al., 2012). Faults on the southern rift could represent the prolongation

of those that are recognisable in the NE area; nevertheless, their exposure on the island's high cliffs requires more precise study

8. Conclusions

The construction of El Hierro Island is the result of the superposition of different constructive and destructive episodes that conditioned occasional changes in the local stress fields. The characteristic radial distribution of structural elements such as dykes and eruptive fissures suggests the existence of a rather uniform stress field during the constructive episodes that was maintained during the growth of the whole island. These radial patterns may result from a combination of loading, gravitational spreading, and magma-induced upwelling, but there is also some influence of previous regional structures. The existence of the well observed NE-SW and N-S directions in the shallower parts of the edifice indicates the presence of a local stress field, possibly conditioned by the formation of giant landslides. These could mask the general radial pattern promoting changes in the uniform stress field and establishing new local stress fields, which would have conditioned the propagation of new intrusions, thereby giving a false impression of the existence of a deep-seated three-armed rift system on El Hierro. Therefore, we propose that the rifts zones described on El Hierro are shallow structures that commonly capture and divert ascending magma towards different parts of the island but do not condition magma ascent at depth.

Acknowledgements

This research was partially funded by IGME, CSIC and the European Commission (FT7 Theme: ENV.2011.1.3.3-1; Grant 282759: "VUELCO"), and MINECO grant GL2011-

16144-E. Michael Lockwood revised and corrected the English text. We would like to thank to the “Consejo Insular de Aguas de El Hierro” for their invaluable help, specially to Juan Manuel Quintero, Jose Miguel Padrón and Pepe Medina who allowed us to visit the water galleries and provided us all their support. A special mention is also for Nicolas Moreau, Daniel de Miguel and Carmen Romero for their assistance in the field work. We also would like to thank to M. Neri and A. Tibaldi for their very valuable suggestions that have enabled us to significantly improve our manuscript.

Figures

Figure 1. Location and simplified geological map of El Hierro Island. Place names in the text are shown on this map. The insets in the top left of the figure show the location of Canary Islands in relation to Europe and Africa and the whole Canary archipelago, where the main tectono-volcanic features and lineations of the archipelago are shown. Each number in the inset refers to the main authors that have studied the regional tectonic setting of the Canaries: (1) Bosshard and McFarlane (1970); Mezcuca et al. (1992); (2) Navarro (1974); (3) Carbó et al. (2003) Simplified geological cross-section at the bottom of the figure shows the superposition of the three volcanic edifices of the island (Modified from IGME, 2010a).

Figure 2. (a) Onshore and offshore vents and (b) volcanic fissures of El Hierro (Modified from Becerril et al., 2013).

Figure 3. Types and morphology of different dykes studied on El Hierro: a) Dykes projection on a DEM; b) simple massive dyke, c) and d) multiple and composite dykes; e) fractured dyke;; f) feeder dyke; g) slight changes in strike of dykes when they pass through materials with different mechanical properties; h) dykes splitting into two branches; i) parallel dykes; j) segmented dyke; k) crossed relationship between dykes.

Figure 4. Dykes and fissures in the Tiñor edifice showing: a) rose diagram and histogram orientations of dykes; b) rose diagram and histogram orientations of fissures; c) histogram showing dyke-dip distribution; d) dyke thickness distribution; e) strike vs. dip; f) strike vs. thickness; e) dip vs. thickness; f) histogram showing fissure length distribution.

Figure 5. Dykes in the El Golfo-Las Playas edifice showing: a) rose diagram and histogram orientations of dykes; b) histogram showing dyke-dip distribution; c) dyke thickness distribution; d) strike vs. dip; e) strike vs. thickness; f) dip vs. thickness.

Figure 6. Dykes and fissures of the Rift Volcanism edifice showing: a) rose diagram and histogram orientations of dykes; b) rose diagram and histogram orientations of fissures; c) histogram showing dyke-dip distribution; d) dyke thickness distribution; e) strike vs. dip; f) strike vs. thickness; e) dip vs. thickness; f) histogram showing fissure length distribution.

Figure 7. Graphics showing main dyke and fissure characteristics of the NE, W and S rifts, both on and offshore. Rose diagrams are presented for dykes in superficial outcrops and also for all water galleries visited. The rose diagrams of fissures are divided into onshore and offshore diagrams.

Figure 8. a) Hillshade map with fault projections and rose diagram of the faults. b) San Andrés fault system. The rose diagram, projection of poles to planes and slickenside projections are also shown; c) outcrop of the graben main fault, known as the San Andrés fault; d) outcrop of the fault affecting Los Picos; e) general view of the Los Picos fault f) topographic profile of the graben system.

Tables

Table 1. Data related to the analysed onshore and offshore vents. TE: Tiñor Edifice; EG-LPE: El Golfo-Las Playas Edifice; RV: Rift Volcanism; EGE: El Golfo Embayment.

Table 2. Data related to the analysed onshore and offshore fissures (See table 1 caption for abbreviations meaning).

Table 3. Data related to the analysed onshore dykes at surface and in water galleries (See table 1 caption for abbreviations meaning).

Table 4. Fault average measurements in sections a, b and c.

References

- Acocella, V., Tibaldi, A., 2005. Dike propagation driven by volcano collapse: A general model tested at Stromboli, Italy. *Geophys. Res. Lett.* 32, 1–4.
- Acocella, V., Porreca, M., Neri, M., Mattei, M., Funiciello, R., 2006. Fissure eruptions at Mount Vesuvius (Italy): insights on the shallow propagation of dikes at volcanoes. *Geology* 34 (8), 673–676
- Ahijado, A., Casillas, R., Hernández-Pacheco, A., 2001. The dyke swarms of the Amanay Massif, Fuerteventura, Canary Islands (Spain). *J. Asian Earth Sci.* 19, 333–345.
- Allmendinger, R. W., Cardozo, N. C., Fisher, D., 2012. *Structural Geology Algorithms: Vectors & Tensors*: Cambridge, England, Cambridge University Press, 289 pp.
- Ancochea, E., Hernán, F., Cendrero, A., Cantagrel, J.M., Fúster, J.M., Ibarrola, E., Coello, J., 1994. Constructive and destructive episodes in the building of young Oceanic Island, La Palma, Canary Islands and genesis of the Caldera de Taburiente. *J. Volcanol. Geotherm. Res.* 60, 243–262.
- Ancochea, E., Brändle, J.L., Cubas, C.R., Hernán, F., Huertas, M.J., 1996. Volcanic complexes in the eastern ridge of the Canary Islands: the Miocene activity of the island of Fuerteventura. *J. Volcanol. Geotherm. Res.* doi:10.1016/0377-0273(95)00051-8
- Ancochea, E., Brändle, J.L., Huertas, M.J., Cubas, C.R., Hernán, F., 2003. The felsic dikes of La Gomera (Canary Islands): Identification of cone sheet and radial dike swarms. *J. Volcanol. Geotherm. Res.* 120, 197–206.
- Ancochea, E., Brändle, J.L., Huertas, M.J., Hernán, F., Herrera, R., 2008. Dike-swarms, key to the reconstruction of major volcanic edifices: The basic dikes of La Gomera (Canary Islands). *J. Volcanol. Geotherm. Res.* 173, 207–216.
- Anderson, E.M., 1936. The dynamics of the formation of cone-sheets, ring dykes and cauldron subsidence. *Proc. Roy. Soc. Edin.* 56, 128–157.
- Anguita, F., Hernan, F., 1975. A propagating fracture model versus a hot spot origin for the Canary Islands. *Earth. Planet. Sc. Lett.* 27, 11–19.
- Anguita, F., Hernan, F., 2000. The Canary Islands: a unifying model. *J. Volcanol. Geotherm. Res.* 103, 1–26.
- Banda, E., Danobeitia, J.J., Surinach, E., Ansorge, J., 1981. Features of crustal structure under the Canary Islands. *Earth. Planet.Sc. Lett.* 55, 11–24. Bartolini, S., Becerril, L., Martí, J. 'Unpublished results'. VERDI: a new Volcanic managEmEnt Risk Database design. *J. Volcanol. Geotherm. Res.*

- Becerril, L. 2009. Approach to volcanic hazard and its effects in coastal areas of the Canary Islands. Master's thesis, Universidad de Las Palmas de Gran Canaria, Spain.
- Becerril, L., Cappello, A., Galindo, I., Neri, M., Del Negro, C., 2013a. Spatial probability distribution of future volcanic eruptions at El Hierro Island (Canary Islands, Spain). *J. Volcanol. Geotherm. Res.* 257, 21–30. doi:10.1016/j.jvolgeores.2013.03.005
- Becerril, L., Galindo, I., Gudmundsson, A., Morales, J.M., 2013b. Depth of origin of magma in eruptions. *Sci. Rep.* 3, 6. doi:10.1038/srep02762
- Borgia, A., Delaney, P.T., Denlinger, R.P., 2000. Spreading volcanoes. *Annu. Rev. Earth. Planet. Sci.* 28, 3409–3412.
- Bosshard, E., MacFarlane, D. J., 1970. Crustal structure of the western Canary Islands from seismic refraction and gravity data, *J. Geophys. Res.* 75, 4901–4918.
- Carracedo, J.C., 1994. The Canary Islands: An example of structural control on the growth of large oceanic-island volcanoes. *J. Volcanol. Geotherm. Res.* doi:10.1016/0377-0273(94)90053-1
- Carracedo, J. C., 1996. Morphological and structural evolution of the western Canary Islands: hotspot-induced three-armed rifts or regional tectonics trends? *J. Volcanol. Geotherm. Res.* 72, 151-162.
- Carracedo, J.C., Day, S., Guillou, H., Rodríguez Badiola, E., Canas, J.A., Pérez Torrado, F.J., 1998. Hotspot volcanism close to a passive continental margin: the Canary Islands. *Geol. Mag.* 135 (5), 591–604.
- Carracedo, J.C., Day, S., Guillou, H., 1999. Giant Quaternary landslides in the evolution of La Palma and El Hierro, Canary Islands. *J. Volcanol. Geotherm. Res.* 94, 169-190.
- Carracedo, J.C., Badiola, E.R., Guillou, H., De La Nuez, J., Pérez Torrado, F.J., 2001. Geology and volcanology of La Palma and El Hierro, Western Canaries. *Estud. Geológicos* 57, 175–273.
- Cappello, A., Neri, M., Acocella, V., Gallo, G., Vicari, A., Del Negro, C. 2012. Spatial vent opening probability map of Mt Etna volcano (Sicily, Italy). *Bull. Volcanol.* 74, 2083-2094.
- Chadwick, W.W., Howard, K.A., 1991. The pattern of circumferential and radial eruptive fissures on the volcanoes of Fernandina and Isabela islands, Galapagos. *Bull. Volcanol.* 53, 259–275.
- Connor, C.B., Condit, C.D., Crumpler, L.S., Aubele, J.C., 1992. Evidence of regional structural controls on vent distribution: Springerville Volcanic Field, Arizona. *J. Geophys. Res.* doi:10.1029/92JB00929

- Coello, J. 1971. Contribución a la tectónica de la isla de El Hierro. *Estudios Geológicos*, 27, 335-340.
- Dañobeitia, J.J., 1988. Reconocimiento geofísico de estructuras submarinas situadas al norte y sur del Archipiélago Canario. *Revista de la Sociedad Geológica de España*, 1, 143–155.
- Day, S.J., Carracedo, J.C., Guillou, H., 1997. Age and geometry of an aborted rift flank collapse: the San Andres fault system, El Hierro, Canary Islands. *Geol. Mag.* doi:10.1017/S0016756897007243
- Delaney, P.T., Pollard, D.D., Ziony, I., Mckee, E.H., 1986. Field relations between dikes and joints: emplacement processes and paleostress analysis 91, 4920–4938.
- Delcamp, A., van Wyk de Vries, B., James, M.R., Gailler, L.S., Lebas, E. 2011. Relationships between volcano gravitational spreading and magma intrusion. *Bull. Volcanol.* doi:10.1007/s00445-011-0558-9
- Delcamp, A., Troll, V.R., van Wyk de Vries, B., Carracedo, J.C., Petronis, M.S., Pérez-Torrado, F.J., Deegan, F.M., 2012. Dykes and structures of the NE rift of Tenerife, Canary Islands: A record of stabilisation and destabilisation of ocean island rift zones. *Bull. Volcanol.* 74, 963–980.
- De La Nuez, J. 1984. El Complejo Intrusivo Subvolcanico de la Caldera de Taburiente (La Palma, Canarias), Ph.D. Thesis, Universidad Complutense de Madrid.
- Dieterich, J.H. 1988. Growth and persistence of Hawaiian volcanic rift zones. *J. Geophys. Res.* 93, 4258–4270.
- Emery, K.O., Uchupi, E., 1984. *The Geology of the Atlantic Ocean*. Springer Verlag, New York. 1050 pp.
- Falsaperla, S., Cara, F., Rovelli, A., Neri, M., Behncke, B., Acocella, V. 2010. Effects of the 1989 fracture system in the dynamics of the upper SE flank of Etna revealed by volcanic tremor data: the missing link?. *J. Geophys. Res.* 115, B11306.
- Feraud, G., Giannerini, G., Campredon, R., Stillman, C. J., 1985. Geochronology of some Canarian dike swarms: contribution to the volcano-tectonic evolution of the archipiélago. *J. Volcanol. Geotherm. Res.*, 25, 29-52.
- Fernández, C., de la Nuez, J., Casillas, R., García Navarro, E. 2002. Stress fields associated with the growth of a large shield volcano (La Palma, Canary Islands). *Tectonics* 21, 13-18. DOI: 10.1029/2000TC900038
- Fiske, R.S., Jackson, E.D., 1972. Orientation and Growth of Hawaiian Volcanic Rifts: The Effect of Regional Structure and Gravitational Stresses. *Proc. R. Soc. A Math. Phys. Eng. Sci.* doi:10.1098/rspa.1972.0115
- Fuster, J.M., 1975. Las Islas Canarias: un ejemplo de evolución temporal y espacial del vulcanismo oceánico. *Estudios Geológicos*, 31, 439–463.

- Fuster, J.M., Hernán, F., Cendrero, A., Coello, J., Cantangrel, J. M., Ancochea, E., Ibarrola, E. 1993. Geocronología de la isla de El Hierro (Islas Canarias). *Boletín de la Real Sociedad Española de Historia Natural. (Geología)*, 88, 86-97.
- Galindo, I., 2005. Estructura volcano-tectónica y emisión difusa de gases de Tenerife (Islas Canarias). Ph.D. thesis, Facultad de Ciencias Geológicas, Universidad de Barcelona, 336 pp.
- Galindo, I., Soriano, C., Martí, J., Pérez, N., 2005. Graben structure in the Las Cañadas edifice (Tenerife, Canary Islands): Implications for active degassing and insights on the caldera formation. *J. Volcanol. Geotherm. Res.* 144, 73–87.
- Galindo, I., Gudmundsson, A., 2012. Basaltic feeder dykes in rift zones: geometry, emplacement, and effusion rates. *Nat. Hazards Earth Syst. Sci.* 12, 3683–3700. doi:10.5194/nhess-12-3683-2012
- Gee, M.J.R., Masson, D.G., Watts, A.B., Mitchell, N.C., 2001a. Offshore continuation of volcanic rift zones, El Hierro, Canary Islands. *J. Volcanol. Geotherm. Res.* 105, 109–119.
- Gee, M.J.R., Watts, A.B., Masson, D.G., Mitchell, N.C., 2001b. Landslides and the evolution of El Hierro in the Canary Islands. *Mar. Geol.* 177, 271–293.
- Geyer, A., Martí, J., 2010. The distribution of basaltic volcanism on Tenerife, Canary Islands: Implications on the origin and dynamics of the rift systems. *Tectonophysics* 483, 310–326.
- Gudmundsson, A., 1995. Infrastructure and mechanics of volcanic systems in Iceland. *J. Volcanol. Geotherm. Res.* 64, 1-22.
- Gudmundsson, A., 2003. Surface stresses associated with arrested dykes in rift zones. *Bull. Volcanol.* 65, 606–619.
- Gudmundsson, A., 2006. How local stresses control magma-chamber ruptures, dyke injections, and eruptions in composite volcanoes. *Earth-Science Rev.* 79, 1-31.
- Guillou, H., Carracedo, J.C., Torrado, F.P., Badiola, E.R., 1996. K-Ar ages and magnetic stratigraphy of a hotspot-induced, fast grown oceanic island: El Hierro, Canary Islands. *J. Volcanol. Geotherm. Res.* doi:10.1016/0377-0273(96)00021-2
- Hausen, H., 1964. Rasgos geológicos generales de la isla del hierro. *Anu. Estud. Atlánticos* 10, 547–593.
- Hernán, F., Vélez, R. 1980. El sistema de diques cónicos de Gran Canaria y la estimación estadística de sus características. *Estud. Geol.* 36, 65-73.
- Hernán, F., Cubas, C. R., Huertas, M. J., Brändle, J. L. y Ancochea, E., 2000. Geometría del enjambre de diques cónicos de Vallehermoso. *La Gomera (Islas Canarias). Geogaceta*, 27, 91-94.

- Hernández-Pacheco, A., Ibarrola, E., 1973. Geochemical variation trends between the different Canary Islands in relation to their geological position. *Lithos*, 6, 389–402.
- IGME, 2010a. Mapa Geológico de España, Escala 1:25.000. Isla de El Hierro. Hoja 1105-II, Valverde, 96 pp.
- IGME, 2010b. Mapa Geológico de España, Escala 1:25.000. Isla de El Hierro. Hoja 1105-III, Sabinosa, 71 pp.
- IGME, 2010c. Mapa Geológico de España, Escala 1:25.000. Isla de El Hierro. Hoja 1105-IV, Frontera, 84 pp.
- IGME, 2010d. Mapa Geológico de España, Escala 1:25.000. Isla de El Hierro. Hoja 1108-I/II, La Restinga, 55 pp.
- Le Bas, M.J., Rex, D.C., Stillman, C.J., 1986. The early magmatic chronology of Fuerteventura, Canary Islands. *Geol. Mag.*, 123, 287–298.
- Longpré, M.A., Chadwick, J.P., Wijbrans, J., Iping, R. 2011. Age of the El Golfo debris avalanche, El Hierro (Canary Islands): New constraints from laser and furnace $^{40}\text{Ar}/^{39}\text{Ar}$ dating. *J. Volcanol. Geotherm. Res.* 203, 76-80.
- Manconi, A., Longpré, M. A., Walter, T. R., Troll, V. R., Hansteen, T. H. 2009. The effects of flank collapses on volcano plumbing system. *Geology*, 37, 1099–1102. doi: 10.1130/G30104A.1
- Marinoni, L.B., Pasquare, Á, G., 1994. Tectonic evolution of the emergent part of a volcanic ocean island: Lanzarote, Canary Islands. *Tectonophysics* 239, 111-135.
- Marinoni, L.B., Gudmundsson, A., 2000. Dykes, faults and palaeostresses in the Teno and Anaga massifs of Tenerife (Canary Islands). *J. Volcanol. Geotherm. Res.* 103, 83–103.
- Martí, J., Ablay, G.J. y Bryan, S., 1996. Comment on “The Canary Islands: an example of structural control on the growth of large oceanic-island volcanoes” by J.C. Carracedo. *J. Volcanol. Geotherm. Res.* 72, 143-149.
- Martí, J., Pinel, V., López, C., Geyer, A., Abella, R., Tárraga, M., Blanco, M.J., Castro, A., Rodríguez, C., 2013. Causes and mechanisms of the 2011-2012 El Hierro submarine eruption (Canary Islands). *J. Geophys. Res.* 118, 823–839. doi:10.1002/jgrb.50087
- Masson, D.G., 1996. Catastrophic collapse of the volcanic island of Hierro 15 ka ago and the history of landslides in the Canary Islands. *Geology*. doi:10.1130/0091-7613(1996)024<0231:CCOTVI>2.3.CO;2
- Masson, D.G., Watts, A.B., Gee, M.J.R., Urgeles, R., Mitchell, N.C., Le Bas, T.P., Canals, M., 2002. Slope failures on the flanks of the western Canary Islands. *Earth-Science Rev.* 57, 1–35.

- McGuire W.J., Pullen A.D., 1989. Location and orientation of eruptive fissures and feeder dykes at Mount Etna; influence of gravitational and regional tectonic stress regimes. *J. Volcanol. Geotherm. Res.* 38, 325-344.
- Mezcua, J., Buforn E., Udías A., Rueda J. 1992. Seismotectonics of the Canary Islands, *Tectonophysics* 208, 447–452.
- Muller, O.H. and Pollard, D.D. 1977. The stress state near Spanish Peaks, Colorado, determined from a dike pattern. *Pure Applied Geophysics*, 115, 69-86.
- Münn, S., Walter, T.R., Klügel, A., 2006. Gravitational spreading controls rift zones and flank instability on El Hierro, Canary Islands. *Geol. Mag.*
doi:10.1017/S0016756806002019
- Nakamura, K., 1977. Volcanoes as possible indicators of tectonic stress orientation - principle and proposal. *J. Volcanol. Geotherm. Res.* 2, 1-16.
- Navarro, J. M. 1974. Estructura geológica de la isla de Tenerife y su influencia sobre la hidrogeología, *Actas del I Congreso Internacional sobre Hidrología en Islas Volcánicas, Lanzarote, Spain*, 13 pp.
- Navarro, A., Soler, C. 1995. El agua en El Hierro. *Cabildo Insular de El Hierro*, 97 p.
- Neri, M., Acocella, V., Behncke, B., Giammanco, S., Mazzarini, F., Rust, D., 2011. Structural analysis of the eruptive fissures at Mount Etna (Italy). *Annals of Geophysics* 54 (5).
- Odé, H. 1957. Mechanical analysis of the dike pattern of the Spanish Peaks area, Colorado. *Bull. Geol. Soc. Am.*, 68, 567-576.
- Paulsen, T.S., Wilson, T.J., 2010. New criteria for systematic mapping and reliability assessment of monogenetic volcanic vent alignments and elongate volcanic vents for crustal stress analyses. *Tectonophysics* 482, 16–28.
doi:10.1016/j.tecto.2009.08.025
- Pellicer, M.J. 1977. Estudio volcanológico de la isla de El Hierro (Islas Canarias). *Estudios Geológicos*, 33, 181-197.
- Pellicer, M.J. 1979. Estudio geoquímico del vulcanismo de la isla de El Hierro, Archipiélago Canario. *Estudios Geológicos*, 35, 15-029.
- Pollard, D.D., Delaney, P.T., Duffield, W.A., Endo, E.T., Okamura, A.T., 1983. Surface deformation in volcanic rift zones. *Tectonophysics*. doi:10.1016/0040-1951(83)90034-3
- Pollard, D.D. 1987. Elementary fracture mechanics applied to the structural interpretation of dykes. In: Halls, H.C. y Faring, W.F. (Eds.), *Mafic dyke swarms*. Geological Association of Canada Special Paper, v. 34: p. 5-24.

- Robertson, A.H.F., Stillman, C.J. 1979. Late Mesozoic sedimentary rocks of Fuerteventura. Canary Islands. Implications for West Africa continental margin evolution. *J. Geol. Soc. London*, 136, 47–60.
- Ryan, M.P. 1988. The Mechanics and Three-Dimensional Internal Structure of Active Magmatic Systems: Kilauea Volcano, Hawaii. *J. Geophys. Res.* 93, 4213-4248.
- Schirnick, C., Bogaard P.V.D., Schmincke H.U. 1999. Cone sheet formation and intrusive growth of an oceanic island: the Miocene Tejeda complex on Gran Canaria (Canary Islands). *Geology*, 27, 207-210.
- Schmincke, H.U., 1967. Cone sheet swarm, resurgence of Tejeda Caldera, and the early geologic history of Gran Canaria. *Bull. Volcanol.* 31, 153-162.
- Schmincke H-U, Graf G (eds), 2000. DECOS/OMEX II, Cruise no. 43, 25 November 1998–14 January 1999. METEORBerichte, Universität Hamburg, 00-2, Universität Hamburg.
- Somoza, L., Vázquez, J.T., González-Aller, D., Dañobeitia, J.J., Medialdea, T., Moya, A.J., Fernández-Salas, L.M., León, R., Jurado, M.J., Paredes, M., Palomino, D., Vargas, I., González, F.J., López-Rodríguez, M., Corbalán, A., González, P., Hernández-Puentes, M.P., Martín-Jiménez, D., 2012. Geophysical and hydroacoustic study of the active submarine volcanism in the El Hierro Island (Canarian Archipelago). VIII Congreso Geológico de España, Oviedo (Spain) on 17–19 July 2012.
- Staudigel, H., Feraud, G., Giannerini, G. 1986. The history of intrusive activity on the island of La Palma (Canary Islands). *J. Volcanol. Geotherm. Res.* 27, 299 –322.
- Stillman, C.J., 1987. A Canary Island Dyke Swarm: implications for the formation of oceanic islands by extensional fissural volcanism. In: Halls, H.C., Fahrig, W.F. Eds, *Mafic Dyke Swarms*. *Geol. Assoc. Can. Spec. Pap.* 34, pp. 243–255.
- Tibaldi, A., 1995. Morphology of pyroclastic cones and tectonics. *J. Geophys. Res.* 100, 24521–24535.
- Tibaldi A., 1996. Mutual influence of diking and collapses at Stromboli volcano, Aeolian Arc, Italy. *Geol. Soc. Spec. Publ.*, London, 110, 55-63.
- Tibaldi A., 2001. Multiple sector collapses at Stromboli volcano, Italy: how they work. *Bull. Volcanology*, 63, 2/3, 112-125.
- Urgeles, R., Canals, M., Baraza, J., Alonso, B., 1996. The submarine “El Golfo” debris avalanche and the Canary debris flow, West Hierro Island: the last major slides in the Canary archipelago. *Geogaceta*, 20, 390-393.
- Urgeles, R., Canals, M., Baraza, J., Alonso, B., Masson, D.G., 1997. The most recent megaslides on the Canary Islands: the El Golfo debris avalanche and the Canary debris flow, west El Hierro Island. *J. Geophys. Res.* 102, 20305-20323.

- van den Bogaard, P., 2013. The origin of the Canary Island Seamount Province—new ages of old seamounts. *Sci. Rep.* 3, 2107. doi:10.1038/srep02107
- Walker, G.P.L., 1992. “Coherent intrusion complexes” in large basaltic volcanoes — a new structural model. *J. Volcanol. Geotherm. Res.* doi:10.1016/0377-0273(92)90036-D
- Walter, T.R., 2003. Buttressing and fractional spreading of Tenerife, an experimental approach on the formation of rift zones. *Geophys. Res. Lett.* doi:10.1029/2002GL016610
- Walter, T.R., Klügel, A., Münn, S., 2006. Gravitational spreading and formation of new rift zones on overlapping volcanoes. *Terra Nov.* 18, 26–33.
- Walter, T.R., Troll, V.R., Cailleau, B., Belousov, A., Schmincke, H.U., Amelung, F., Bogaard, P., 2005. Rift zone reorganization through flank instability in ocean island volcanoes: An example from Tenerife, Canary Islands. *Bull. Volcanol.* 67, 281–291.

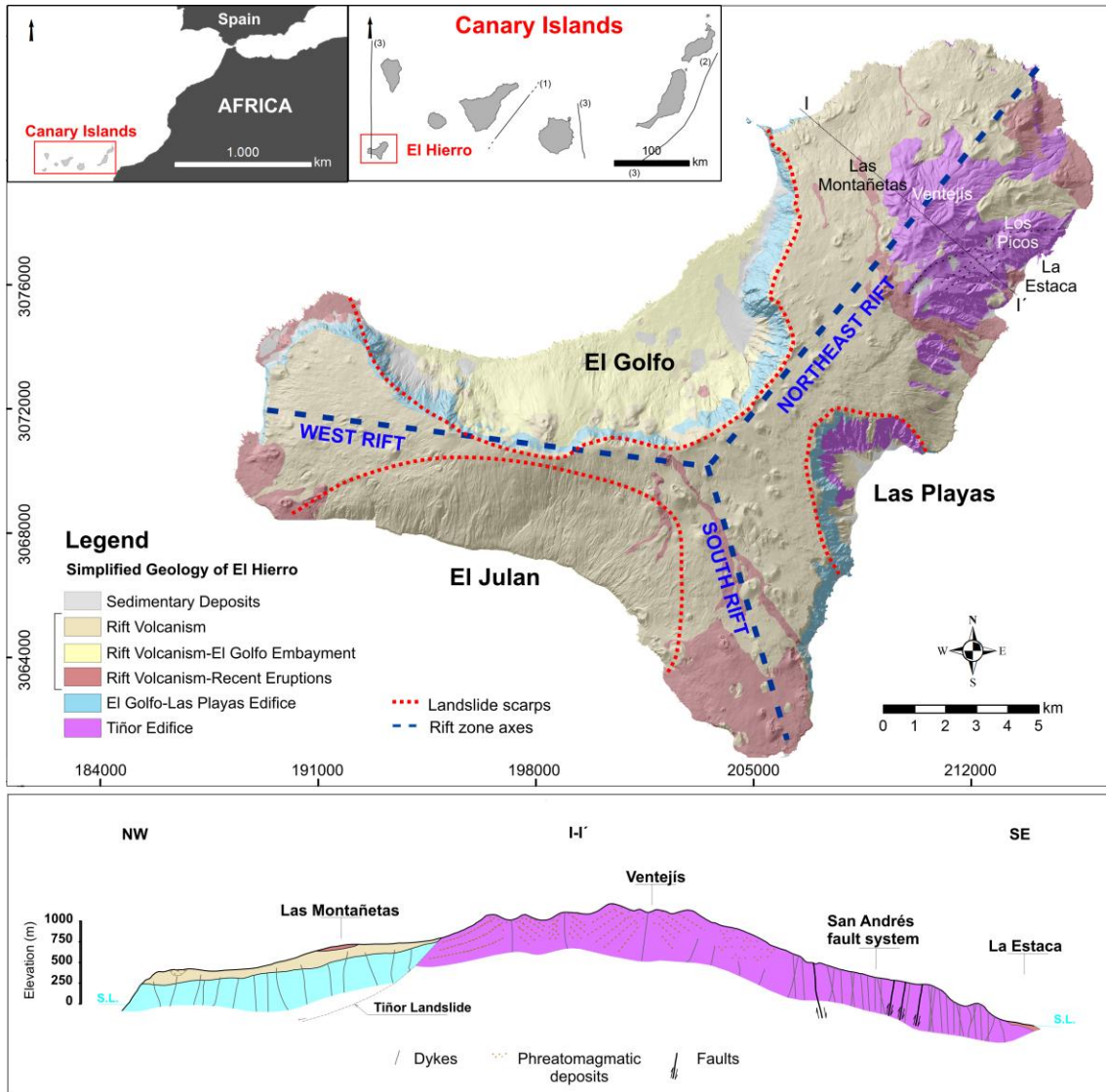


Figure 1

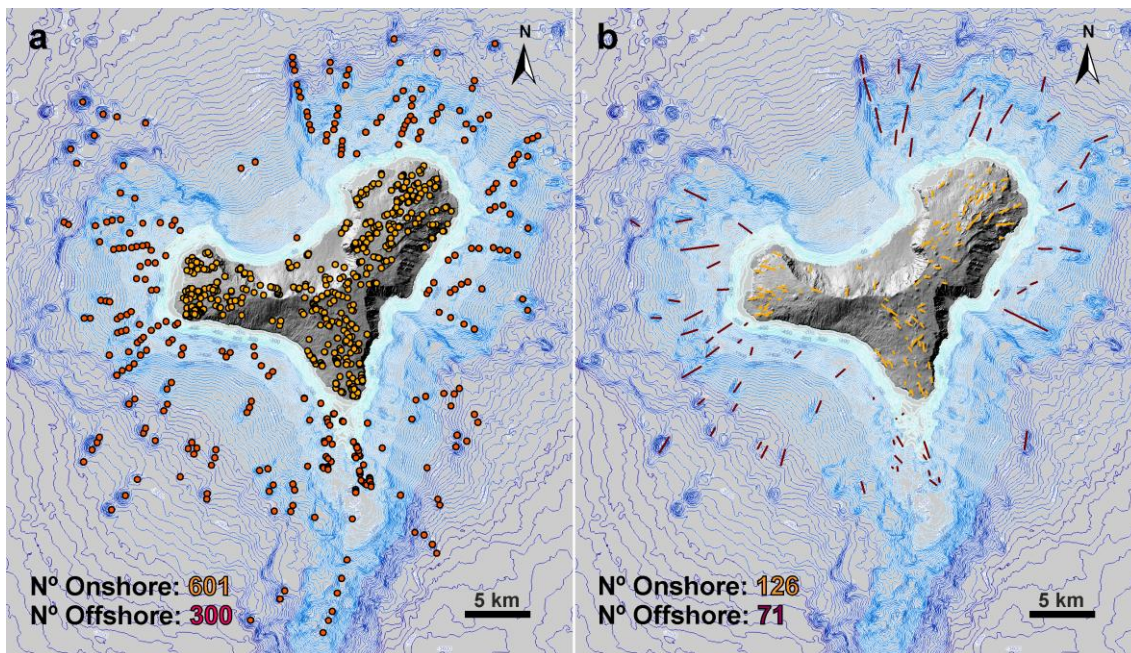


Figure 2

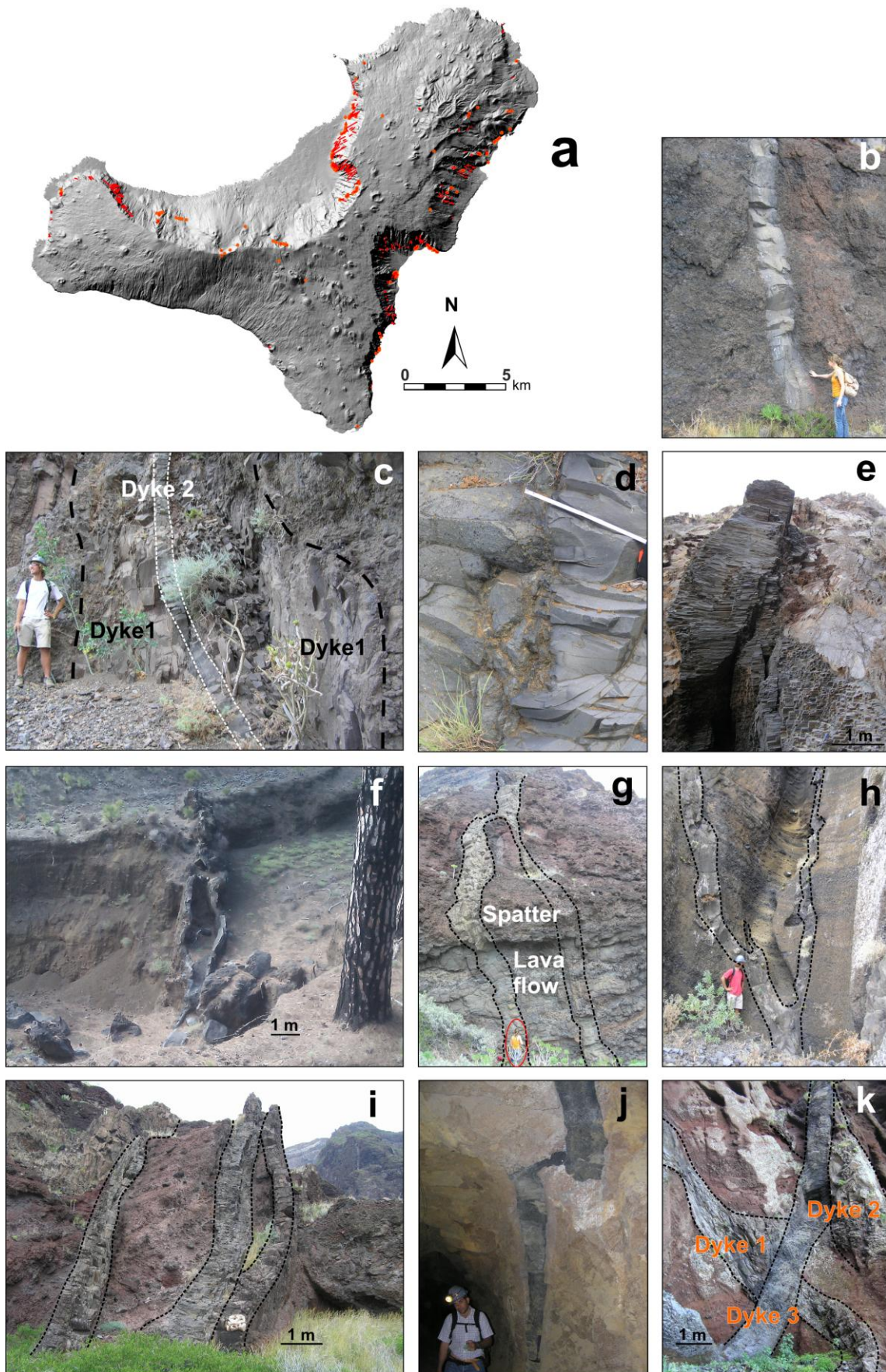


Figure 3

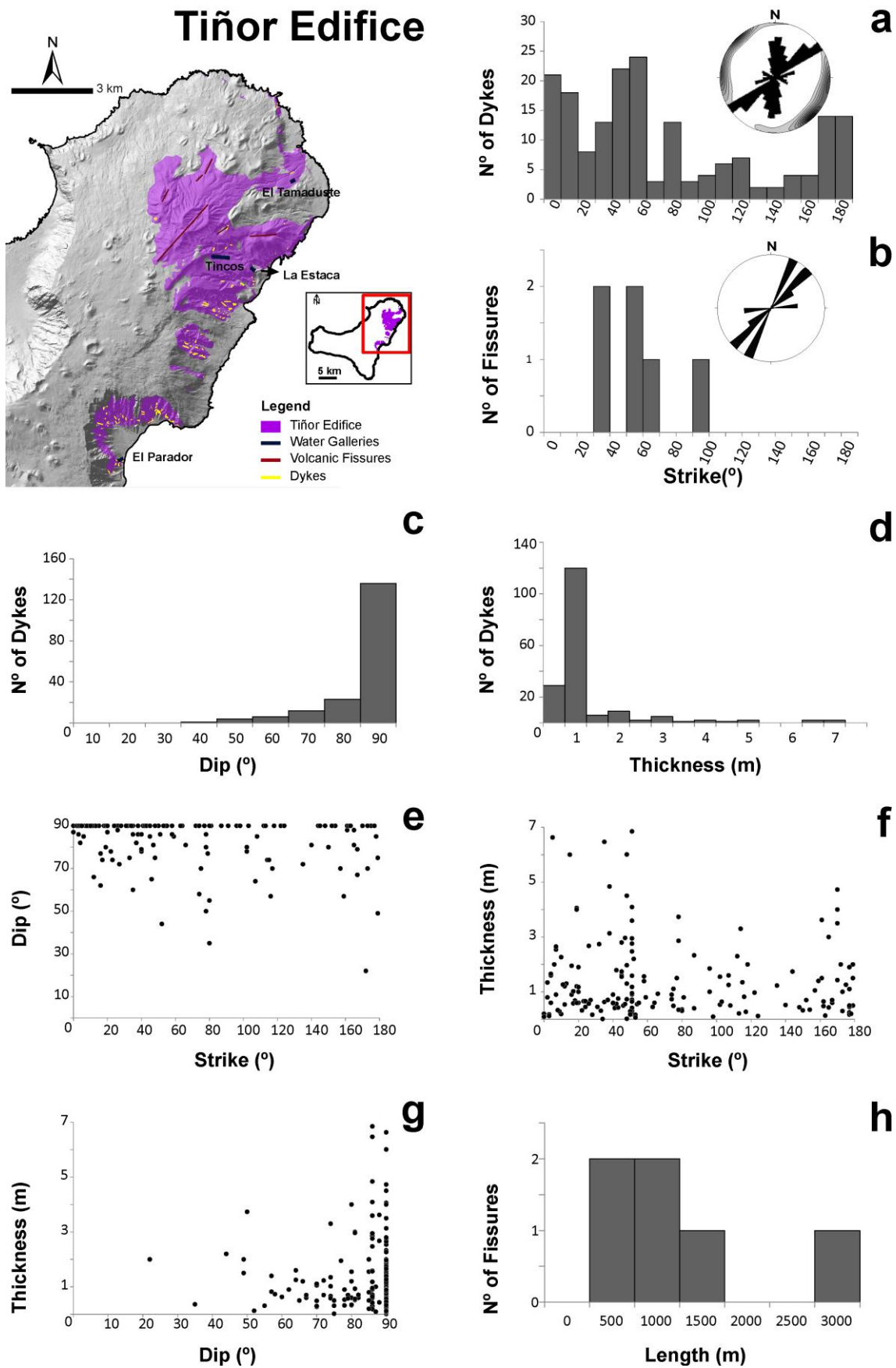


Figure 4

El Golfo-Las Playas Edifice

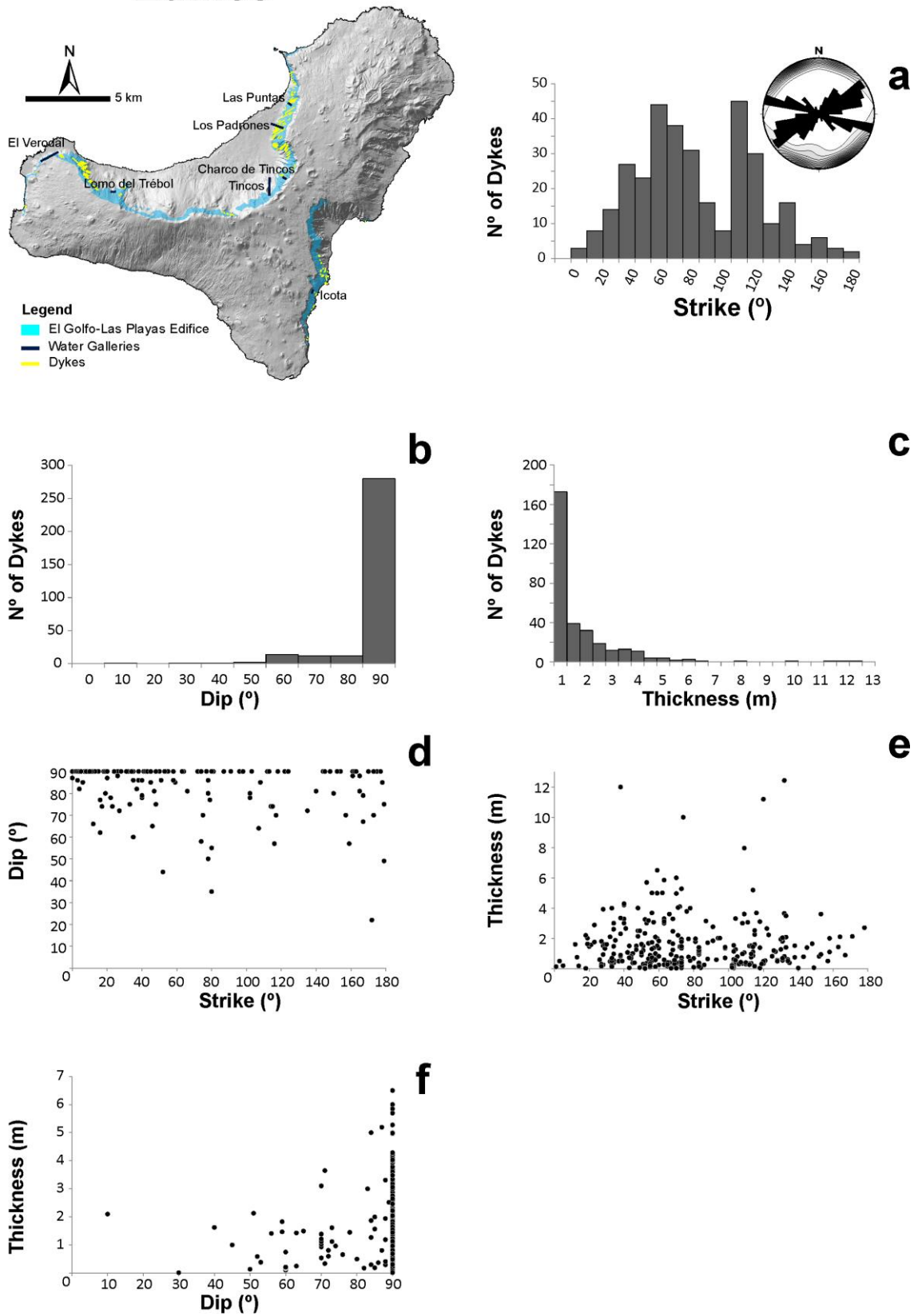


Figure 5

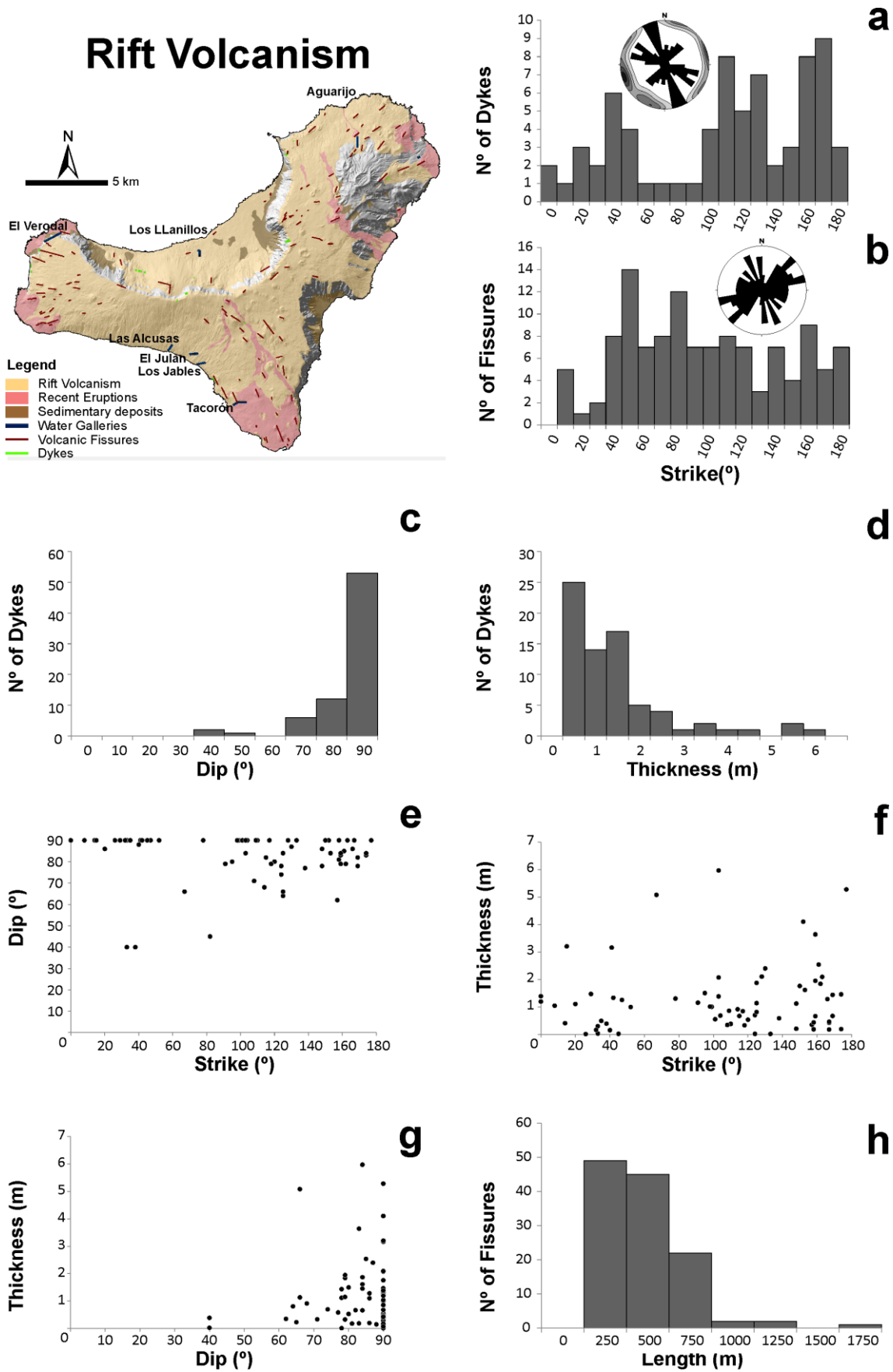


Figure 6

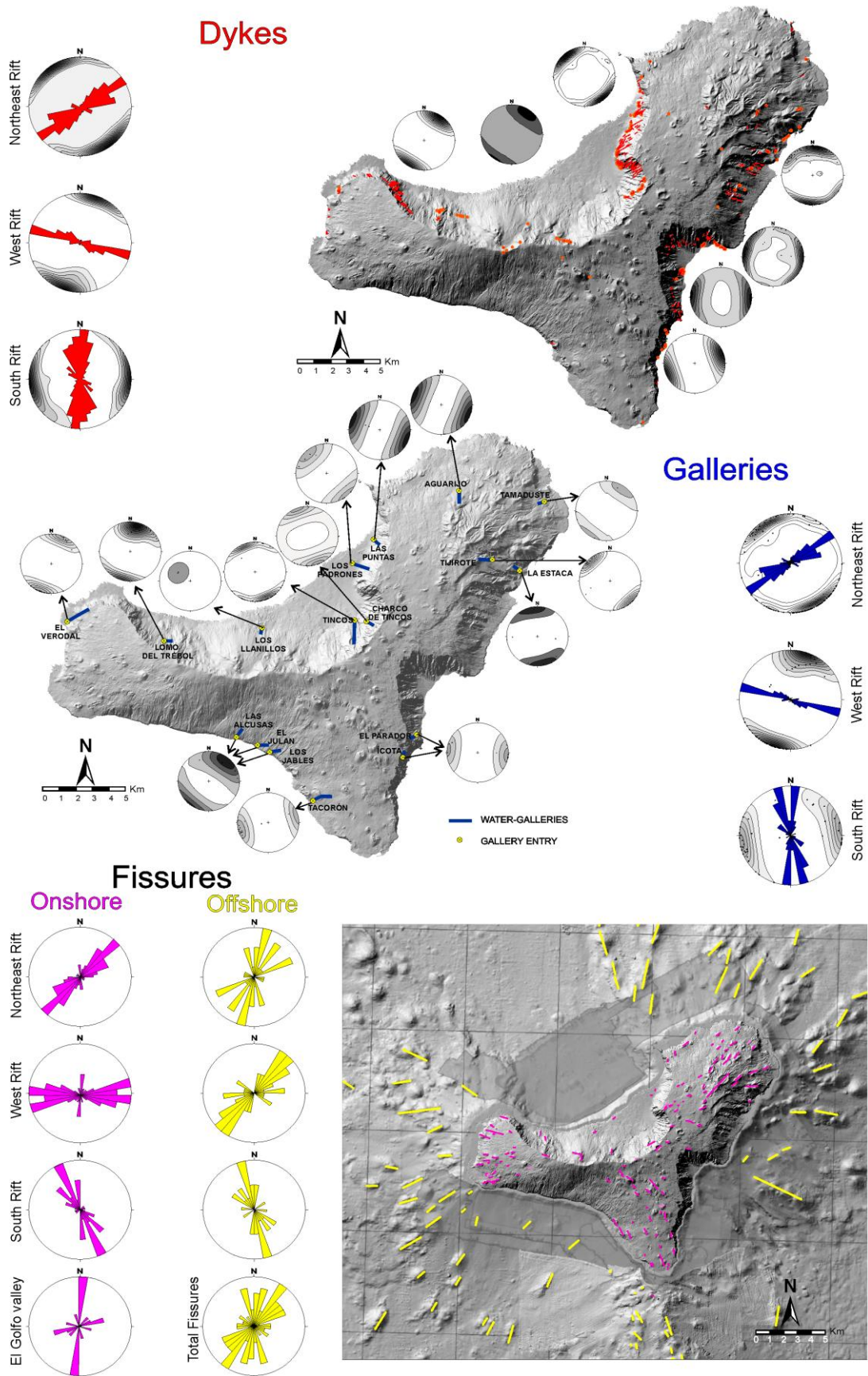


Figure 7

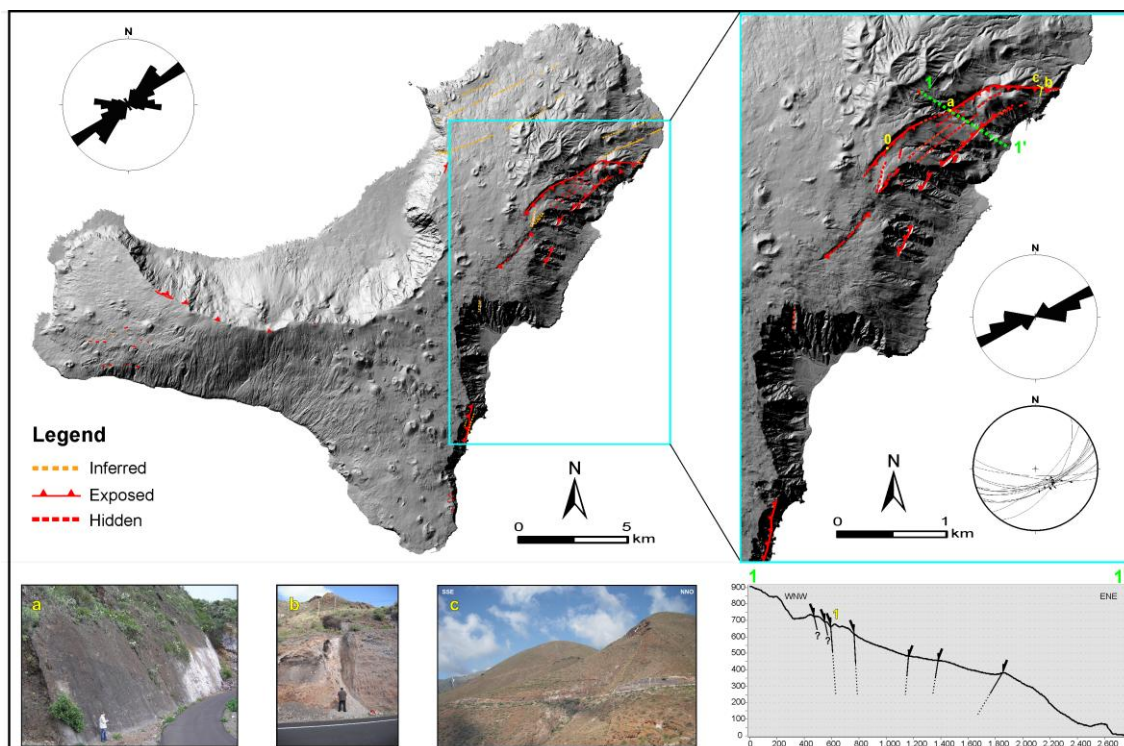


Figure 8

Table 1.

		EDIFICE			LOCATION				TOTAL
		TE	EG-LPE	RV	NE	S	W	EGE	
ONSHORE	N°	33	1	567	213	174	162	52	601
	%	5.5	0.16	94.34	35.45	28.95	26.95	8.65	100
OFFSHORE	N°	NO AVAILABLE DATA DUE TO THE LACK OF AGES			96	93	108	3	300
	%	NO AVAILABLE DATA DUE TO THE LACK OF AGES			32	31	36	1	100

Table 2.

		EDIFICE			LOCATION				TOTAL						
		TE	EG-LPE	RV	NE	S	W	EGE							
ONSHORE	N°	6	-	121	56	34	31	5	126						
	%	4.72	-	95.27	44.44	26.98	24.60	3.96	100						
	Strike average	N47°E	-	N107°E	N52°E	N89°E	N145°E	N50°E N130°E N180°E	-						
	Length (m)(min/max)	338	2825	-	38	1557	41	2825	38	1108	83	1557	232	734	-
	N° of Vents (min/max)	2	4	-	2	33	2	8	2	8	2	33	2	4	408
OFFSHORE	N°				26	29	16	-	71						
	%				37	41	22	-	100						
	Strike average	NO AVAILABLE DATA DUE TO THE LACK OF AGES			N61°E	~NNE-SSW	N161°E	-	-						
	Length (m)(min/max)				575	4603	66	1738	302	3651	-	-	-		
	N° of Vents (min/max)				2	5	2	7	2	7	-	-	183		

Table 3.

Cycle	Dykes at surface			Dykes in water galleries		
	TE	EG-LPE	RV	TE	EG-LPE	RV
N°	105	119	27	78	209	49
%	57	36	34	43	64	66
Strike average (°)	N40-60°E N170-180°E	N60°-80°E N110°-140°E	N40°-50°E N100°-130°E N160-180°E	N40-60°E N170-180°E	N60°-80°E N110°-140°E	31-118- 166
Dip average (°)	81	86.1	83	85.7	86.5	82
Thickness average (m)	1.30	1.86	1.52	1.60	1.34	1.10

Table 4.

Fault Section	Strike	Dip	Groove Trend	Plunge
a	040	65° SE	135°	65°
b	067	65° SE	130°	62°
c	090	72° S	139°	60°

HIGHLIGHTS

- The first comprehensive volcano-tectonic model of El Hierro
- New analysis of the structural elements: vents, eruptive fissures, dykes and faults
- Structural-element distribution suggests uniform stress field during construction
- Shallow NE, S, and W rifts indicate local stress fields conditioned by landslides